Eur. Phys. J. D **2**, 231–235 (1998)

THE EUROPEAN PHYSICAL JOURNAL D

Calculation of dielectronic recombination cross sections and rate coefficients for heliumlike carbon

J.-G. Wang[1,a], T.-Q. Chang[1], and Y.-Z. Qu[2]

[1] Institute of Applied Physics and Computational Mathematics, P.O. Box 8009, Beijing 100088, P.R. China
[2] Institute of Physics, Chinese Academy of Sciences, P.O. Box 603, Beijing 100080, P.R. China

Received: 7 July 1997 / Revised: 7 October 1997 / Accepted: 8 December 1997

Abstract. A simplified relativistic configuration interaction method is used to calculate the dielectronic recombination cross sections and rate coefficients for heliumlike carbon. In this method, the infinite resonant doubly excited states can be treated conveniently in the frame of Quantum Defect Theory. Our calculated cross sections are in agreements with the experimental measurements except for the $1s2lnl'(n = 6, 7)$ resonances. The total energy-integrated cross sections and rate coefficients over all dielectronic resonances are in agreements with the experimental measurements within 10% percent.

PACS. 34.80.Kw Electron-ion scattering; excitation and ionization – 34.80.Dp Atomic excitation and ionization by electron impact

1 Introduction

Dielectronic recombination (DR) can be regarded as a resonant radiative recombination process. As a free electron with a specific kinetic energy collides with an ion A^{q+}, one of the bound electrons of the ion A^{q+} is excited from $n_a l_a$ orbital into $n_r l_r$ orbital, at the same time, the free electron is captured into an unoccupied orbital nl and forms a resonant doubly excited state; subsequently, the resonant doubly excited state decays into a non-autoionizing state through radiative transition processes. Its importance in influencing the ionic balance in high temperature plasmas has been known for many years [1]. Since then, many theoretical methods have been developed, such as distorted wave method [2,3], close coupling methods [4,5], non-relativistic single- and multi-configuration [6–9] and relativistic multi-configuration methods [10,11]. In these calculations, it is difficult to obtain the DR rate coefficients since they involve many resonant doubly excited high Rydberg states. Quantum Defect Theory (QDT) has been developed to treat the atomic processes involving high Rydberg states [12–14], and was also used to study the DR cross sections and rate coefficients for high Rydberg states by extrapolation [15–17]. In the frame of Quantum Defect Theory (QDT), we have developed a simplified relativistic configuration interaction (SRCI) method. In this method, all the resonant doubly excited high Rydberg states can be treated in a unified manner by interpolation (rather than extrapolation), and then the DR cross sections and rate coefficients can be obtained conveniently. We have calculated the DR cross sections of the hydrogen-like ions [18–20], and the results are in good agreement with the experimental measurement [21,22]. In the present paper, the SRCI method is extended to study the DR processes of heliumlike carbon ion. As an impurity, the carbon ion can induce the radiative cooling of magnetically confined plasma, and as a few-electron system, the heliumlike carbon ion is usually a testing ground for theoretical DR calculations, so there exist a lot of theoretical and experimental works on the DR processes of heliumlike carbon ion [23–30]. Recently, Kilgus *et al.* [31] measured the cross sections of the processes with a high resolution at the heavy-ion storage ring TSR, and their theoretical calculations reproduced well the experimental cross sections, except in a region extending about 5 eV below the almost degenerate excitation thresholds $1s2s(^1S)$ and $1s2p(^3P)$. In this energy region, the resonant doubly excited states can autoionize to the excited states of the initial recombining ion, namely, the Coster-Kronig channel is open [26,32], which cause a new difficulty for theoretical calculations. In this paper, using our SRCI method, we also studied this DR process. The theoretical cross section and rate coefficients are presented and compared with the experimental measurements, which is regarded as a testing of our theoretical method.

2 Theoretical method

The DR process of heliumlike carbon has the form

$$e^- + \mathrm{C}^{4+}(1s^2) \longleftrightarrow \mathrm{C}^{3+}(1sn_r l_r nl)^{**} \rightarrow \mathrm{C}^{3+}(1s^2 n_k l_k)^* + h\nu. \quad (1)$$

[a] e-mail: jslcp@mail.iapcm.ac.cn

In the present paper, we study the DR processes for the doubly excited states with $n_r = 2$. For the $1s2pnl$ doubly excited Rydberg states, the Coster-Kronig transition $1s2pnl \rightarrow 1s2s + e^-$ becomes energetically possible for certain large n [26–30,32] , which is included in our calculation. The cross section of a resonant capture process, in which the C^{4+} ion in initial state $i(1s^2)$ or $i(1s2s)$(Coster-Kronig transition) captures a free electron with a specific energy ϵ_i and forms the C^{3+} atom in the resonant doubly excited state $j(1sn_rl_rnl)$, can be treated in the isolated resonance approximation (atomic unit is used throughout unless specified),

$$\sigma_{ij}^c = \frac{\pi^2\hbar^3}{m_e\epsilon_i}\frac{g_j}{2g_i}A_{ji}^a\delta(\epsilon-\epsilon_i), \tag{2}$$

where g_i and g_j are the statistical weight of the state i and j, respectively. A_{ji}^a is the Auger decay rate (inverse resonant capture), which can be calculated using the Fermi golden rule.

We construct the configuration wavefunctions $\phi(\Gamma JM)$ (Γ denotes the quantum numbers $1sn_rl_rnl$ and parity) as anti-symmetrized product-type wavefunctions from central-field Dirac orbitals with appropriate angular momentum coupling [33]. All relativistic single-electron wavefunctions (bound and continuum) are calculated based on the atomic self-consistent potential [34,35]. An atomic state function for the state $j(1sn_rl_rnl)$ with total angular momentum JM is then expressed as linear superposition of the configuration wavefunctions with the same principal quantum numbers (n_r, n) and orbital angular momentum quantum numbers (l_r, l)

$$\psi_j(JM) = \sum_{\lambda=1}^{m} C_{j\lambda}\phi(\Gamma_\lambda JM). \tag{3}$$

Here m is the number of the configuration wavefunctions, and the mixing coefficients $C_{j\lambda}$ for state j are obtained by diagonalizing the relevant Hamiltonian matrices [33]. The SRCI is much simpler than the relativistic multi-configuration methods [10,11]. It has included the main configuration interactions and is better than the relativistic single-configuration interaction methods. When (n_r,l_r,l) are fixed and n varies from bound to continuum state, all the resonant doubly excited states with the same J and coupling scheme will form a channel. In our SRCI method, the channels can be easily classified, and the transition matrix elements in the channels can be conveniently calculated by interpolation (rather than extrapolation).

The free state is chosen as the single configuration wavefunction. Then we have

$$A_{ji}^a = \frac{2\pi}{\hbar}|\sum_{\lambda=1}^{m} C_{j\lambda}M_{ij\lambda}^a|^2, \tag{4}$$

where the Auger decay matrix element $M_{ij\lambda}^a$ is defined as

$$M_{ij\lambda}^a = <\phi(\Gamma_\lambda JM)|\sum_{s<t}\frac{1}{r_{s,t}}|\Psi_{i\epsilon_i}> . \tag{5}$$

In the channel, the energy-normalized matrix element can be defined as

$$\overline{M}_{ij\lambda}^a = M_{ij\lambda}^a(\nu_n^{3/2}/q), \tag{6}$$

here (ν_n^3/q^2) is the density of state [36], $\nu_n = n - \mu_n$, and μ_n is the corresponding quantum defect. This energy-normalized matrix element $\overline{M}_{ij\lambda}^a$ varies smoothly with the electron orbital energy in the channel [19,20]. When the energy-normalized matrix elements of a few states (including one continuum state) in a channel have been calculated, the Auger decay matrix elements of infinite discrete states of that channel can be obtained by interpolation. On the other hand, the mixing coefficients $C_{j\lambda}$ in (4) are almost unchanged whithin a channel [19,20]. We can use the mixing coefficients of a state with a certain high principal quantum number to approximate that of those states with higher principal quantum number. From the expression (4), the Auger rates and capture rates (by detailed balance) of the infinite resonant doubly excited states can be obtained conveniently.

The resonant doubly excited state may autoionize with a rate A_{ji}^a by reemitting an Auger electron or decay radiately into a lower energy state k with a radiatively rate A_{jk}^r, which is defined as

$$A_{jk}^r = \frac{4e^2\omega}{3\hbar c^3 g_j}|\sum_{\lambda,\lambda'=1}^{m,m'} C_{j\lambda}C_{k\lambda'}M_{jk}^r|^2, \tag{7}$$

where ω is the photon energy, the radiative transition matrix element is defined as

$$M_{jk}^r = <\phi(\Gamma_\lambda JM)|T^{(1)}|\phi'(\Gamma'_\lambda J'M')> \tag{8}$$

and here $T^{(1)}$ is the electronic dipole operator [33].

For the radiative process with certain final state $k(1sn_kl_k)$, the resonant doubly excited states with the fixed (n_r, l_r, l) and different orbital energy form a channel. In the channel, the energy-normalized radiative transition matrix element is defined as

$$\overline{M}_{jk}^r = M_{jk}^r(\nu_n^{3/2}/q). \tag{9}$$

This energy-normalized matrix element varies slowly with the electron orbital energy [19,20]. By interpolation, all the energy-normalized matrix elements of infinite discrete states in a channel can be obtained. From the expression (7), we can obtain all the radiative rates in the channel [37, 38].

The resonance energy ϵ_i can be calculated under the frozen core approximation [39]. Then, we can obtain the DR cross sections for any resonant doubly excited states conveniently,

$$\begin{aligned}\sigma_{ij;k} &= \frac{\pi^2\hbar^3}{m_e\epsilon_i}\frac{g_j}{2g_i}\frac{A_{ji}^aA_{jk}^r}{\sum_{k'}A_{jk'}^r + \sum_{i'}A_{ji'}^a}\delta(\epsilon-\epsilon_i)\\ &\equiv S_{ij,k}\delta(\epsilon-\epsilon_i).\end{aligned} \tag{10}$$

Here the summation i' is over all possible Auger final states of C^{3+} (j), and the summation k' is over all possible

states of C^{3+} whose energy are below state j. $\delta(\epsilon-\epsilon_i)$ is a delta function. $S_{ij,k}$ is the DR strength. If the energy distribution of the incident electron is Maxwellian, the DR rate coefficient can be written as,

$$\alpha^{DR}_{ij;k} = (\frac{2\pi\hbar^2}{m_e\kappa T})^{3/2}\frac{g_j}{2g_i}\frac{A^a_{ji}A^r_{jk}}{\sum_{k'}A^r_{jk'}+\sum_{i'}A^a_{ji'}}e^{-\frac{\epsilon_i}{\kappa T}}. \quad (11)$$

Here κ is the Boltzmann constant and T is the temperature of the electron. The total rate coefficient can be written as $\alpha^{DR}_i = \sum_{j,k}\alpha^{DR}_{ij;k}$.

In order to compare with the experimental results, the calculated cross section should be convoluted with a Gaussian distribution with an energy resolution Γ. The convoluted cross section is

$$\sigma^{DR}_t(\epsilon) = \sum_j \frac{S_{ij;k}}{\sqrt{2\pi}\Gamma}\exp[-\frac{(\epsilon-\epsilon_j)^2}{2\Gamma^2}]. \quad (12)$$

In this work, the experimental resolution width 2.1 eV (FWHM) is adopted.

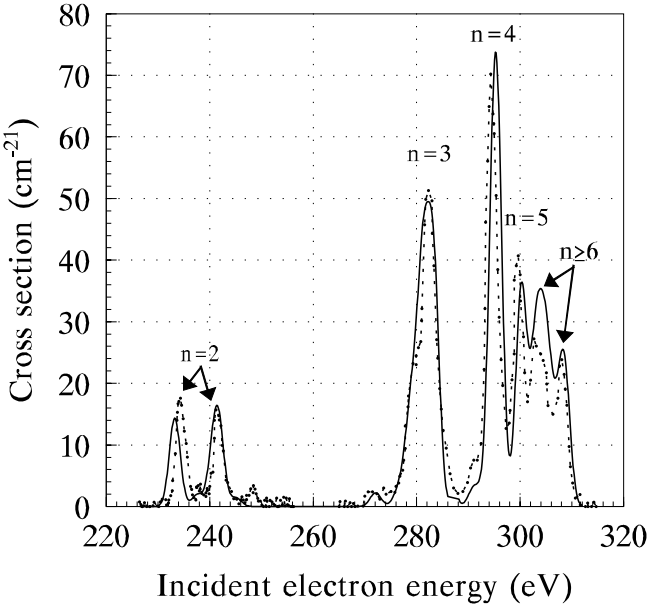

Fig. 1. The DR cross sections of heliumlike carbon for the $1s2lnl'(n=3,4,5,...\infty)$ resonances. Full line: the convoluted theoretical cross sections; Dashed line: Kilgus *et al.*'s experimental cross sections [31].

3 Results and discussion

Using the above SRCI method, we have studied the DR processes for Heliumlike carbon and obtained the cross sections and corresponding rate coefficients. The calculated cross sections and the comparison with Kilgus *et al.*'s experimental measurements [31] are shown in Figure 1. As the principal quantumn n of the resonances $1s2lnl'(n=2,3,4)$ increases, the peaks of the cross sections increase. These features are similar to that of the low Z hydrogenlike DR [20], which is different from the behavior of mediate Z hydrogenlike DR [19], and don't have the n^{-3} scaling relation. The reason is as following: for the low Z ion, $A^a \gg A^r$, we have $\sigma^{DR} \propto \frac{A^a_{ji}\sum_k A^r_{jk}}{\sum_{k'}A^r_{jk'}+\sum_{i'}A^a_{ji'}} \sim \sum_k A^r_{jk}$ (Coster-Kronig transition is neglected). For the doubly excited states $1s2lnl'$, the main radiative contributions come from the transition $1s2lnl' \to 1s^2nl'$, which is independent on the principal quantum number n. So the n^{-3} scaling relation can't be retained. Compared with the experimental measurements [31], the positions and strengths of our calculated peak are in general agreements with the measurements. Looking at the details, for the $1s2l2l'$ resonances, the peak with lower energy is a little less than the peak with higher energy, which is in accordence with Bellantone *et al.*'s single calculations [28] and Beigman *et al.*'s Z expansion calculations [31], but it is different from Kilgus *et al.*'s experimental measurements and calculations [31]. This may be due to the smaller mixed configuration number included in our SRCI, Bellantone *et al.*'s and Beigman *et al.*'s calculations.

Because of the effects of angular momentum coupling and configuration interaction, the resonances $1s2lnl'$ are split into many sublevels. For $n \geq 5$, we find that some sublevels are open for the $2^3S\epsilon l$ Coster-Kronig channel(non-relativistic notations have been used), while others are closed; for $n=8$ resonances, some sublevels are open for the $2^1S\epsilon l$ Coster-Kronig channel; for $n>8$ resonances, some sublevels are open for the $2^3P\epsilon l$ Coster-Kronig channel. In Figure 1, there exists a "valley" near the $n=9$ resonances, which is very different from the smooth high-n behavior of the DR cross section for mediate Z heliumlike ion [26,40]. This is because the $2^3P\epsilon l$ Coster-Kronig channel is opened. Our calculated DR cross sections for the $1s2lnl'(n=6,7)$ resonances, as well as the theoretical results in reference [31], are significantly larger than the experimental measurements [31], which will be discussed after the integrated cross sections are compared with experiments.

Our energy-integrated resonance strengths and comparison with other theoretical and experimental results are displayed in Table 1. Because of the effect of the Coster-Kronig channel, the energy-integrated resonance strengths for $1s2lnl'$ resonances decrease rapidly with n as $n>5$. But the contribution from the high Rydberg resonances ($n \geq 9$) to total energy-integrated resonance strengths is still as large as about 10%. Also, the n^{-3} scaling relation is not retained in this case. So, a proper method to treat the high Rydberg resonances, such as our SRCI method, is needed. Compared with Kilgus *et al.*'s experiments [31], our calculations for the $1s2lnl'(n=6,7)$ resonances, which give a little improvement over Kilgus *et al.*'s theoretical results [31], still overestimate the energy-integrated resonance strengths. The reason may be as following: the appearances of Coster-Kronig channels increase the calculated difficulties for Auger rates, which may be one reason for overestimating cross sections. Not including the bound-continuum and continuum-continuum configuration interactions may be another reason. Since the

Table 1. The energy-integrated strengths (10^{-21}cm^{2}eV) for DR of C^{4+} *via* resonances $1s2lnl'$.

n	Theory[a]	Theory[b]	Theory[c]	Theory[d]	Expt.[b]
2	95.8	96.2	102.9	93.2	89(2)
3	264.4	274.9	188.6	282.8	260(4)
4	218.4	223.0	163.3		227(4)
5	97.8	110.2	57.5		97(2)
6	68.5	81.8			47(2)
7	58.3	69.0			33(2)
8	18.6	18.6			21(4)
≥ 9	80.4	90.8			75(4)
Total	902.2	964.5	784.4		849(8)

[a]Present work
[b]Kilgus *et al.* [31]
[c]Bellantone *et al.* [28]
[d]Beigman *et al.* [31], Vainshtein *et al.* [23]

Auger electron energy is near zero for the Coster-Kronig channels, it is hard to determine the appearance of the Coster-Kronig channels and to calculate the Auger rates with high accuracy. This may introduce numerical errors in our calculations of DR processes. The configuration interactions (bound-bound,bound-continuum and continuum-continuum), not included in our SRCI method, may introduce an inaccuracy in our calculation.

The total energy-integrated cross sections over all dielectronic resonances are in agreement with the experimental measurements within 10% percent, as shown in Table 1. We also calculated the total rate coefficients, which are related directly to the total energy-integrated cross sections, and compare them with other theoretical works [31,28,26] and experimental measurements [31] as shown in Figure 2. Although there exists a relatively large error for the $1s2lnl'(n = 6, 7)$ resonances, our calculated rate coefficients are in agreement with the experimental measurements within 10% percent.

It should be noted that because of the configuration interaction and other effects not considered in our calculations, the individual transition probabilities A^a and A^r and even a few cross sections such as the $1s2lnl'(n = 6, 7)$ resonances may not be accurate, but our calculated total energy-integrated cross sections and rate coefficients are in agreement with the experimental measurements within 10% percent. This is because the errors and variations in the calculations of the individual transition probabilities tend to cancel in the evaluation of DR cross sections and rate coefficients, and total energy-integrated cross sections and rate coefficients are not too sensitive to errors made in the calculation of individual transition probabilities [17,41]. The calculated accuracy for rate coefficents in our SRCI method can be sufficient for most practical applications. Due to the fully relativistic treatments in our calculation, our SRCI method can also be used to study the DR processes for high Z elements, which will be discussed in other future papers.

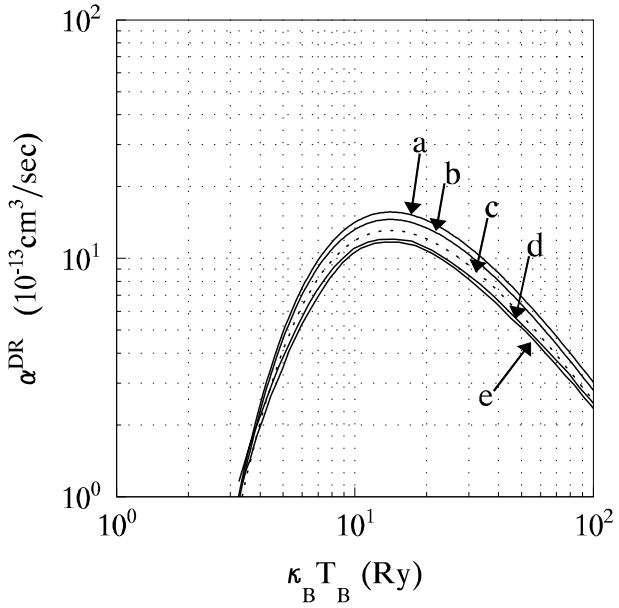

Fig. 2. The total rate coefficients of heliumlike carbon for the $1s2lnl'(n = 3, 4, 5, ...\infty)$ resonances. a: Kilgus *et al.*'s theoretical results [31]; b: Present theoretical results; c: experimental results obtained by the cross sections digited from Kilgus *et al.*'s work [31]; d: Bellantone *et al.*'s theoretical results [28]; e: Chen's theoretical results [26].

The authors would like to express their gratitude to Prof. Jia-Ming Li and Prof. Chen-Zhong Dong for their helpful discussions. This work was supported by National Natural Science Foundation of China, Pos. Doc. Foundation of China and National Youth Foundation of High Tech.

References

1. A. Burgess, Astrophys. J. **139**, 776 (1964).
2. W. Eissner, M.J. Seaton, J. Phys. B: At. Mol. Phys. **6**, 2187 (1972).
3. D.R. Flower, J.M. Launay, J. Phys. B: At. Mol. Phys. **5**, L207 (1972).
4. H.E. Saraph, M. J. Seaton, Phil. Trans. Roy. Soc. A **271**, 1 (1971).
5. J. Dubau, Ph.D. Thesis, University of London, 1973.
6. Y. Hahn, Phys. Rev. A **22**, 2896 (1980).
7. D.J. McLaughlin, Y. Hahn, Phys. Rev A **29**, 712 (1984).
8. N.R. Badnell, J. Phys. B **19**, 3827 (1986).
9. N.R. Badnell, M.S. Pindzola, Phys. Rev. A **39**, 1685 (1989).
10. M.H. Chen, Phys. Rev. A **31**, 1449 (1985).
11. H.P. Saha, Phys. Rev. A **49**, 894 (1994).
12. D.R. Bates, A. Damgaard, Philos. Trans. R. Soc. London **242**, 101 (1949).
13. M.J. Seaton, Proc. Phys. Soc. Lond. **88**, 801 (1966); Rep. Prog. Phys. **46**, 167 (1983).
14. C.M. Lee (Jia-Ming Li), K.T. Lu, Phys. Rev. A **8**, 1241 (1973) .
15. J. Dubau, J. Wells, J. Phys. B **2**, 1452 (1973).
16. M.J. Seaton, P.J. Storey, 1976, in *Atomic processes and applications*, edited by P.G. Burke and B.L. Moiseiwitsch, (North-Holland Publishing Company) p. 133.

17. Y. Hahn, Adv. At. Mol. Phys. **21**, 123 (1985).
18. C.-Z. Dong, Y. Zou, J.-G. Wang, J.-M. Li, Acta Phys. Sinica V **44**, 1712 (1995).
19. J.-G. Wang, Y. Zou, C.-Z. Dong, J.-M. Li, Chin. Phys. Lett. V **12**, 530 (1995).
20. J.-G. Wang, Y.-Z. Qu, J.-M. Li, Phys. Rev. A **52**, 4274 (1995).
21. D.R. DeWitt, D. Schneider, M.W. Clark, M.H. Chen, Phys. Rev. A **44**, 7185 (1991).
22. D.R. DeWitt, R. Schuch, T. Quinteros, H. Gao, W. Zong, H. Danared, M. pajek, N.R. Badnell, Phys. Rev. A **50**, 1257 (1994).
23. L.A. Vainshteinand, U.I. Safranova, At. Data Nucl. Data Tables **21**, 49 (1978); **25**, 311 (1980).
24. F. Bely-Dubau, J. Dubau, P. Faucher, L. Steenman-Clark, J. Phys. B **14**, 3313 (1981).
25. S.M. Younger, J. Quant. Spectrosc. Radiat. Transfer **29**, 67 (1983)
26. M.H. Chen, Phys. Rev. A **38**, 6430 (1988).
27. Y. Hahn, K.J. LaGattutta, Phys. Rep. **166**, 195 (1988).
28. R. Bellantone, Y. Hahn, Phys. Rev. A **40**, 6913 (1989).
29. Y. Hahn, Phys. Scr. T **28**, 25 (1989).
30. N.R. Badnell, M.S. Pindzola, D.C. Griffin, Phys. Rev. A **41**, 2422 (1990).
31. G. Kilgus, D. Habs, D. Schwalm, A. Wolf, R. Schuch, N.R. Badnell, Phys. Rev. A **47**, 4859 (1993).
32. V.L. Jacobs, J. Davis, P.C. Kepple, M. blaha, Astrophys. J. **211**, 605 (1977).
33. Z.-X. Zhao, J.-M. Li, Acta Physica Sinica **34**, 1469 (1985).
34. J.-M. Li, Z.-X. Zhao, Acta Physica Sinica **31**, 97 (1982).
35. D.A. Liberman, D.T. Cromer, J.T. Waber, Comput. Phys. Commun. **2**, 107 (1971) .
36. C.M. Lee (Jia-Ming Li), W.R. Johnson, Phys. Rev. A **22**, 975 (1980).
37. L. Liu, J.-M. Li, Acta Phys. Sinica V **42**, 1901 (1993).
38. J.-G. Wang, X.-M. Tong, J.-M. Li, Acta Phys. Sinica V **45**, 13 (1996).
39. C.M. Lee, Phys. Rev. A **10**, 584 (1974).
40. P. Beiersdorfer, M.B. Schneider, M. Bitter, S. von Goeler, Rev. Sci. Instrum. **63**, 5029 (1992).
41. Y. Hahn, Rep. Prog. Phys. **60**, 691 (1997).